

Electronic Supplementary Material

Hin et al. (2013): Experimental evidence for Mo isotope fractionation between metal and silicate liquids

S.1 Mo concentration analyses by laser ablation ICPMS

Molybdenum concentrations in silicates of selected samples were analysed by laser ablation ICPMS (LA-ICPMS; Table S1). The purpose of these analyses was to investigate the feasibility of isotopic analyses, but the obtained data are provided for comparison with concentrations obtained from double spiked isotope ratio analyses (MC-ICPMS). The samples RH75, RH91 and RH93 were analysed by LA-ICPMS, but not by MC-ICPMS. Samples that are presented in Table 3 of the main manuscript but lacking in Table S1 were only analysed by MC-ICPMS.

Analyses by LA-ICPMS were performed with a Geolas excimer laser with a wavelength of 193 nm, coupled to a quadrupole ICPMS (Perkin Elmer Elan 6100 DRC). The laser was operated at 15 Hz with a spot size of $\sim 40 \mu\text{m}$ and an energy fluence of $\sim 12 \text{ J cm}^{-2}$. Ablated material was transported from the sample cell to the ICP torch by a N_2 flux. The NIST SRM610 glass standard was analysed before and after each sample to correct for mass bias drift. All analyses were internally normalised to CaO concentrations determined by electron microprobe analyses, except for samples RH86 and RH87. For their analyses, internal normalisation to FeO concentrations was found to be most satisfactory due to heterogeneity in other oxide concentrations as a result of large olivine quench needles.

As can be seen in Table S1 and Figure S1, average Mo concentrations determined by LA-ICPMS generally match well with bulk Mo concentrations determined by MC-ICPMS. This confirms that the careful metal-silicate separation procedure involving centrifugation, sawing, polishing, crushing and microscopic inspection produced metal-free silicate pieces for analyses by MC-ICPMS.

S.2 Double spike calibration

We have added a ^{100}Mo - ^{97}Mo double spike to our samples prior to digestion to correct for instrumental mass bias as well as potential mass dependent isotope fractionation during chemical separation. Both ^{97}Mo -enriched and ^{100}Mo -enriched metal powders were purchased from the Oak Ridge National Laboratory (Batch number ^{100}Mo 159992, Batch number ^{97}Mo 159791). After dissolution, their isotopic compositions and concentrations were determined relative to an in-house gravimetric Mo standard (Mo metal powder from Alfa Aesar; LOT number C24P28). The optimum double spike mixture was then determined from the abundances of the single spikes using the 'double spike toolbox' of Rudge et al (2009).

The gravimetrically prepared double spike was subsequently analysed for its isotopic composition and corrected for instrumental mass bias by bracketing with a Mo standard. The instrumental fractionation factor in the bracketing standards was determined by internal normalisation to a $^{97}\text{Mo}/^{95}\text{Mo}$ ratio of 0.602083 (Lu and Masuda, 1994). The isotopic composition of the same Mo standard was also internally normalised to provide the isotopic composition of the reference standard in the double spike deconvolution. This calibration was initially performed on Nu1700 at ETH Zurich against the in-house Mo standard (Alfa Aesar). In an attempt to establish an international reference standard (Greber et al., 2012), however, the calibration was repeated on a Neptune Plus (Münster) against the NIST SRM 3134 Mo standard relative to which all previously performed analyses have been recalculated.

The results of these calibration procedures have been verified with double spike – standard mixtures with various proportions of double spike ranging from 0.185 to 0.806, with 0.477 as an optimum spike proportion. No trends of isotopic compositions are observed as a function of double spike proportion, confirming the accuracy of the calibration (Figure S2).

Table S1. LA-ICPMS concentration data for Mo. Except RH86 and RH87, all data were internally normalised to CaO concentrations determined by EPMA. RH86 and RH87 were internally normalised to FeO, because of heterogeneity in other oxide concentrations due to large olivine quench needles. Uncertainties for Mo concentrations determined by MC-ICPMS are estimated, because it was difficult to estimate weighing errors for samples $< 20 \text{ mg}$ and these are probably the main source of uncertainty. n = number of repeated analyses.

Sample	[Mo] (ppm) LA-ICPMS	SD	n	[Mo] (ppm) MC-ICPMS ¹
RH55	44.3	2.4	4	52.5
RH77	42	20	3	58.2
RH86	127	48	4	108
RH87	269	108	4	193
RH92	45.4	5.4	3	52.6
RH94	6.1	0.8	3	9.61
RH97	6.3	5.3	3	6.09
RH98	7.3	4.0	3	7.61
RH99	11.3	7.7	3	11.0
RH75	5.1	0.6	3	n.d.
RH93	111.4	0.5	3	n.d.

¹ Relative uncertainty (SD) better than 1%.

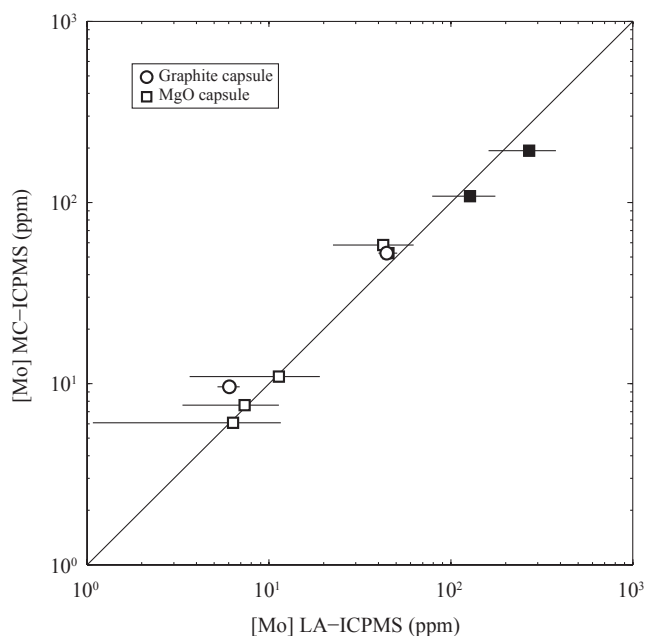


Figure S1. Silicate melt Mo concentrations determined by isotope ratio analyses plotted against concentrations determined by LA-ICPMS. The methods agree well. Error bars for LA-ICPMS data are 1SD; those for concentrations determined by MC-ICPMS are consistently smaller than symbol sizes.

References:

Greber, N.D., Siebert, C., Nägler, T.F., Pettke, T., 2012. $\delta^{98/95}\text{Mo}$ values and molybdenum concentration data for NIST SRM 610, 612 and 3134: Towards a common protocol for reporting Mo data. *Geostand Geoanal Res.* 36, 291-300.
 Lu, Q., Masuda, A., 1994. The isotopic composition and atomic weight of Molybdenum. *Int J Mass Spectrom* 130, 65-72.
 Rudge, J.F., Reynolds, B.C., Bourdon, B., 2009. The double spike toolbox. *Chem. Geol.* 265, 420-431.

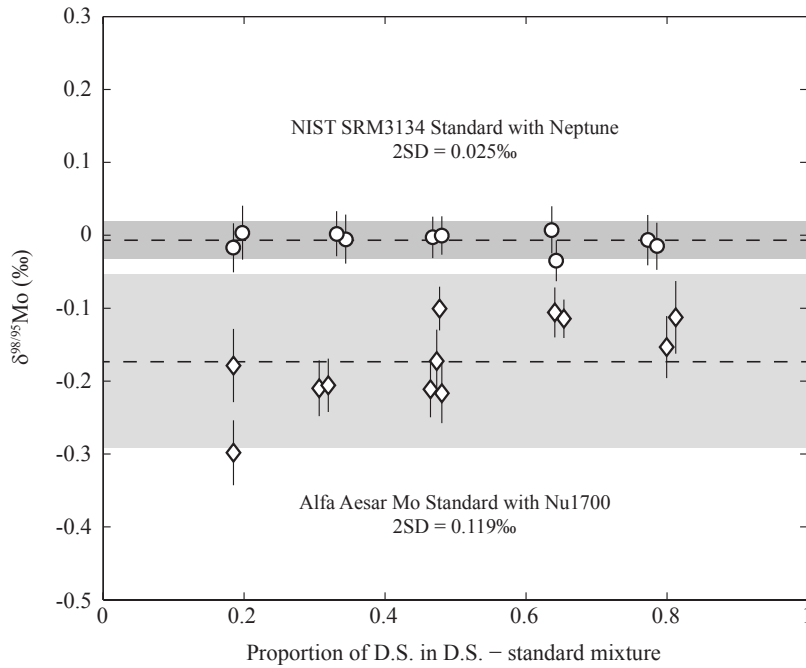


Figure S2. Plot of $\delta^{98/95}\text{Mo}$ against spike proportion in various double spike – standard mixtures. The isotopic compositions are shown for mixtures with two different standards: the in-house Alfa Aesar Mo standard on Nu1700 (Zurich; diamonds) and NIST SRM 3134 on Neptune Plus (Münster; circles). Isotopic compositions are independent of spike proportions in either data set, confirming the accuracy of the double spike and standard calibrations. Individual error bars are 2SE internal errors.

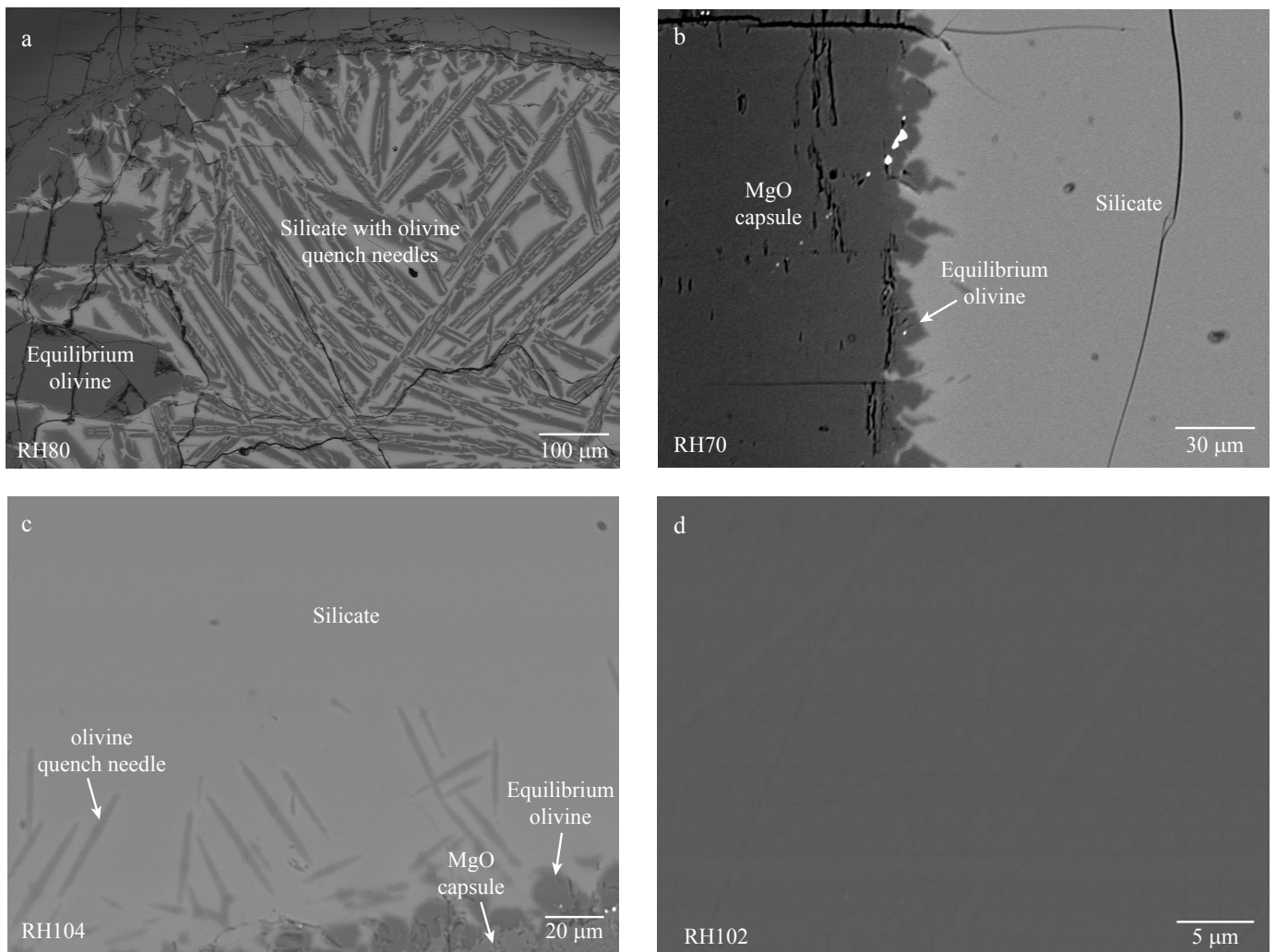


Figure S3. Backscattered electron images of selected experiments. Panel (a) presents the equilibrium olivine and relatively large olivine quench needles in experiments performed in MgO capsules at 1600°C, while panels (b) and (c) show the much smaller (<25 μm) and much less abundant equilibrium olivine crystals in experiments performed in MgO capsules at 1400°C. Note also that no metal is visible in the silicate glasses in panels (b) and (c). The absence of tiny metal droplets in silicate glass is also shown in panel (d).

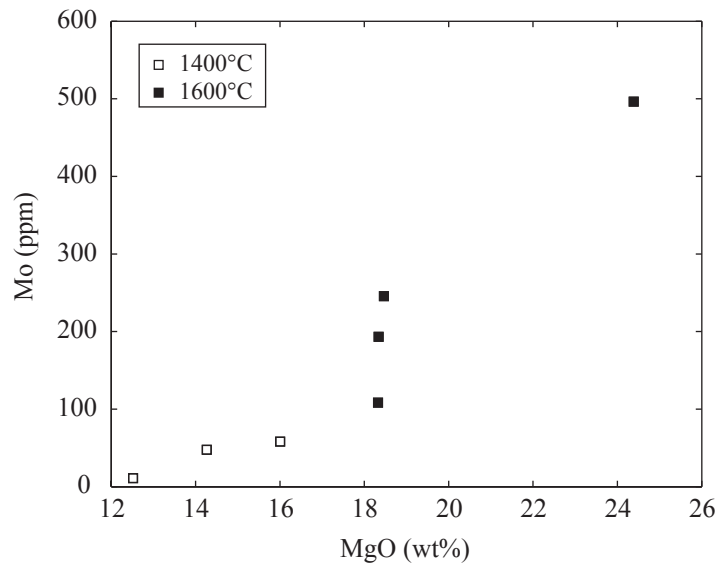


Figure S4. Molybdenum content against MgO content. The presented data are from experiments performed in MgO capsules at an oxygen fugacity of ΔIW -0.64 to -0.73. All errors (2SD) are smaller than twice the symbol sizes.

Table S2. Elemental compositions (wt%) of all samples with their experimental run conditions. The silicate compositions of experiments run in MgO capsules take into account the glass and quench crystals, euhedral crystals were not taken into account. P = pressure (GPa), T = temperature (°C), f_{O_2} = oxygen fugacity relative to the iron-wüstite buffer (ΔIW), t = run duration in hour.

	Start Mix A			Start Mix B1			Start Mix B2			Start Mix C										
	RH55	2SD	RH71	2SD	RH72	RH74	2SD	RH76	2SD	RH77	2SD	RH82	2SD	RH94	2SD	RH97	2SD	RH98	2SD	
P (GPa) ¹	0.79	0.10	1.06	0.10	0.91	0.08	0.73	0.17	0.82	0.07	0.90	0.05	0.91	0.06	0.97	0.03	0.98	0.04	1.00	0.07
T (°C)	1400		1400		1400		1400		1400		1400		1400		1400		1400		1400	
t (h)	4.0		0.5		1.5		4.0		7.0		4.0		2.2		1.7		1.5		1.5	
f_{O_2} (ΔIW)	0.10		0.16		0.14		0.14		0.13		-0.70		-0.64		-1.05		-1.68		-1.71	
Capsule type	Graphite		Graphite		Graphite		Graphite		Graphite		MgO		MgO		Graphite		MgO		MgO	
Metal jacket	Pt		Au ₅₀ Pd ₅₀		Au ₅₀ Pd ₅₀		Au ₅₀ Pd ₅₀		Au ₅₀ Pd ₅₀		Au ₅₀ Pd ₅₀		Pt		Pt		Pt		Pt	
Metal																				
Fe	71.6	3.0	70.9	3.7	73.2	1.7	75.4	3.7	81.1	0.9	64.0	10.1	67.8	4.8	70.0	1.9	68.9	1.5	68.6	2.0
Sn	15.8	4.1	14.5	2.8	12.5	1.1	8.79	5.19	1.46	0.34	23.7	8.8	22.8	4.2	15.5	2.0	21.1	0.4	21.4	1.1
Mo	8.38	1.05	10.4	2.0	9.86	1.00	10.7	3.1	11.6	0.7	9.65	1.89	9.81	1.83	10.2	1.1	10.2	1.5	9.90	0.89
Pt	n.a.	n.a.	n.a.	n.a.	n.a.	n.a.	n.a.	n.a.	n.a.	n.a.	n.a.	n.a.	0.09	0.12	0.05	0.05	0.06	0.04	0.08	0.06
Pd	n.a.	n.a.	0.07	0.14	0.14	0.13	0.33	1.05	0.23	0.15	2.00	2.19	n.a.	n.a.	n.a.	n.a.	n.a.	n.a.	n.a.	n.a.
Total	95.8	1.2	95.8	0.9	95.7	0.4	95.2	1.2	94.4	0.5	99.4	0.8	100.6	1.2	96.0	0.8	100.5	0.7	100.2	0.9
C (calc) ²	4.2		4.2		4.3		4.8		5.6		4.0									
Silicate																				
SiO ₂	42.9	0.7	43.0	1.7	42.8	1.1	43.1	0.9	43.6	0.4	45.5	4.8	46.0	5.7	48.6	0.7	45.8	0.9	45.2	0.9
Al ₂ O ₃	3.92	0.26	2.45	0.24	2.47	0.13	2.43	0.12	2.46	0.10	1.78	0.79	1.67	0.68	7.73	0.38	7.25	0.21	7.19	0.23
MgO	3.92	0.20	3.05	0.21	3.10	0.18	3.12	0.13	3.14	0.11	16.0	11.1	14.3	8.9	8.01	0.34	14.4	0.4	14.8	0.6
FeO	32.8	0.9	36.7	0.7	37.1	0.6	37.1	1.3	38.7	0.5	27.2	2.5	28.6	5.6	9.59	0.32	8.71	0.39	8.38	0.49
CaO	10.6	0.1	9.61	0.34	9.55	0.26	9.56	0.38	9.76	0.20	8.22	5.57	7.27	4.88	17.3	0.4	16.7	0.7	16.6	0.9
Na ₂ O	0.96	0.11	0.98	0.18	0.97	0.13	0.98	0.13	0.98	0.07	0.63	0.36	0.56	0.34	3.94	0.20	3.66	0.26	3.66	0.21
K ₂ O	0.00	0.01	0.00	0.02	0.00	0.01	0.00	0.01	0.00	0.01	0.25	0.08	0.24	0.12	0.98	0.07	0.92	0.15	0.91	0.15
SnO ₂	3.57	0.23	3.04	1.27	3.03	0.95	2.40	0.44	0.73	0.21	0.74	0.51	1.14	0.84	0.74	0.31	0.26	0.10	0.22	0.07
Total	98.6	0.8	98.8	0.8	99.0	1.1	98.7	2.4	99.4	0.8	100.4	1.3	99.7	1.6	96.9	1.0	97.8	0.8	97.0	1.1

¹ Errors refer to the time dependent variation of the pressure in centrifuge experiments. They are calculated as the 2SD of the pressure registrations in 30 s intervals in our log files.

² Carbon contents are calculated as the difference of the totals from 100%.

³ Owing to the larger olivine quench crystals occurring in experiments in MgO capsules at 1600 °C, the silicate composition of this sample is derived from a mass balance calculation based on the analysed compositions of the olivine quench crystals and the glassy matrix.

Table S2, continued.

	Start Mix C		Start Mix D		Start Mix E		Start Mix B2						Start Mix F							
	RH104	2SD	RH101	2SD	RH99	2SD	RH80 ³	2SD	RH87 ³	2SD	RH92	2SD	RH103	2SD	RH81 ³	2SD	RH86 ³	2SD	RH102	2SD
P (GPa) ¹	0.91	0.04	0.95	0.04	0.89	0.05	1.00	0.04	1.06	0.08	0.98	0.08	0.95	0.17	0.98	0.04	0.95	0.02	0.10	0.09
T (°C)	1400		1400		1400		1600		1600		1600		1600		1600		1600		1600	
t (h)	4.0		1.7		1.5		1.1		0.7		1.7		1.4		1.1		0.8		1.2	
fO ₂ (ΔIW)	-1.79		0.47		-0.52		-0.70		-0.62		0.12		0.06		-0.72		-0.73		0.06	
Capsule type	MgO		Graphite		MgO		MgO		MgO		Graphite		Graphite		MgO		MgO		Graphite	
Metal jacket	Pt		Pt		Pt		Pt		Pt		Pt		Pt		Pt		Pt		Pt	
Metal																				
Fe	68.9	2.1	73.8	0.5	72.4	5.1	67.4	10.1	66.5	9.6	73.0	1.1	73.2	1.2	92.8	4.0	89.2	4.6	85.4	0.8
Sn	20.5	1.3	9.04	0.43	26.2	5.3	23.0	11.2	22.6	8.3	12.3	1.2	12.7	0.6	n.a.	n.a.	n.a.	n.a.	n.a.	n.a.
Mo	10.3	0.9	11.8	0.5	1.66	0.13	9.63	3.04	10.9	2.3	9.67	0.88	9.43	0.86	7.50	3.68	9.79	4.22	9.21	0.76
Pt	0.09	0.09	0.01	0.03	0.04	0.05	0.13	0.24	0.09	0.10	0.04	0.05	0.03	0.04	0.11	0.13	0.10	0.09	0.04	0.05
Pd	n.a.		n.a.		n.a.		n.a.		n.a.		n.a.		n.a.		n.a.		n.a.		n.a.	
Total	100.0	0.9	94.9	0.4	100.3	0.4	100.2	1.1	100.3	1.1	95.3	0.9	95.6	0.7	100.4	0.9	99.3	0.6	94.8	1.1
C (calc) ²			5.1							4.7			4.4						5.2	
Silicate																				
SiO ₂	46.2	0.5	39.9	0.8	42.4	5.6	37.6	1.5	40.6	2.7	47.7	2.2	48.2	2.1	37.7	1.6	38.5	0.9	46.9	0.6
Al ₂ O ₃	7.14	0.22	1.22	0.12	1.65	0.94	1.79	0.55	1.89	0.80	1.83	0.10	1.77	0.15	2.64	0.68	2.45	1.19	1.97	0.12
MgO	16.4	1.0	0.85	0.10	12.5	11.3	24.4	6.2	18.3	5.2	1.25	0.13	1.21	0.08	18.5	4.8	18.3	4.0	1.32	0.09
FeO	7.89	0.36	49.0	1.6	32.5	4.8	26.6	6.4	28.7	7.8	34.5	1.8	33.8	1.3	30.8	5.0	30.4	5.1	40.4	0.6
CaO	16.8	1.2	3.39	0.42	7.91	6.92	7.75	1.63	8.93	1.17	7.91	0.21	8.00	0.19	9.54	1.48	9.62	0.74	8.05	0.19
Na ₂ O	3.64	0.12	0.83	0.12	0.66	0.43	0.65	0.20	0.65	0.10	0.62	0.11	0.64	0.10	0.94	0.29	0.86	0.24	0.64	0.10
K ₂ O	0.86	0.12	0.01	0.02	0.27	0.11	0.28	0.08	0.24	0.07	0.24	0.07	0.24	0.04	0.33	0.11	0.33	0.17	0.23	0.03
SnO ₂	0.21	0.09	4.06	0.39	0.94	0.77	1.07	0.46	1.27	0.24	4.36	0.64	4.39	0.76	0.00	0.00	0.01	0.02	0.00	0.00
Total	99.1	0.7	99.2	1.3	98.8	1.7	100.1	0.9	100.7	0.9	98.4	0.9	98.2	0.7	100.3	0.7	100.4	0.7	99.5	0.9